Supporting Information

S1. Characterization of OCL diblock copolymers

Table S1. Characterization of PEO-*b*-PCL diblock copolymers

Polymer OCL (X,Y)	MW of PEO (g/mole)	MW of PCL (g/mole)	MW of OCL (g/mole)	M_{CH_2} (g/mole)	f_{EO}	PDI by GPC	Morphology
OCL (1, 0.5)	1000	540	1540	388	0.75		monomers
OCL (1, 1)	1000	966	1966	695	0.65		loose aggregates
OCL (1, 3)	1000	3067	4067	2206	0.46		vesicles
OCL (1, 4)	1000	4100	5100	2949	0.42		vesicles
OCL (1, 6)	1000	6315	7315	4543	0.38		vesicles
OCL (1, 12)	1000	12444	13444	8951	0.33	1.48	precipitates
OCL (2, 3)	2000	2900	4900	2086	0.57	1.23	spheres
OCL (2, 6)	2000	5900	7900	4244	0.46	1.6	vesicles, worms
OCL (2, 7)	2000	7080	9080	5092	0.44	1.45	worms, vesicles
OCL (2, 8)	2000	8020	10020	5769	0.42	1.51	worms, vesicles
OCL (2, 9)	2000	9000	11000	6474	0.41	1.42	worms, vesicles
OCL (2, 10)	2000	10100	12100	7265	0.40	1.52	worms, vesicles
OCL (2, 11)	2000	11200	13200	8056	0.39	1.65	worms, vesicles
OCL (2, 12)	2000	11900	13900	8560	0.38	1.6	worms, vesicles
OCL (2, 13.5)	2000	13000	15500	9800	0.37	1.46	worms, vesicles
OCL (2, 15)	2000	15500	17500	11149	0.36	1.57	precipitates
OCL (2, 18)	2000	18613	20613	13388	0.35		precipitates
OCL (3.5, 4)	3500	3954	7454	2844	0.62		wpheres
OCL (3.5, 9)	3500	9155	12655	6585	0.48	1.55	wpheres
OCL (3.5, 12)	3500	12628	16128	9083	0.44		vesicles, spheres
OCL (3.5, 16)	3500	16395	19895	11793	0.41		vesicles, spheres
OCL (5, 3)	5000	2952	7952	2123	0.73		spheres
OCL (5, 6)	5000	5900	10900	4244	0.61	1.4	spheres
OCL (5, 9)	5000	8755	13755	6297	0.54		spheres, vesicles
OCL (5, 10)	5000	10511	15511	7561	0.51	1.6	vesicles, spheres
OCL (5, 11)	5000	11093	16093	7979	0.50		vesicles
OCL (5, 12)	5000	11700	16700	8416	0.49		vesicles
OCL (5, 18)	5000	17900	22900	12875	0.44		vesicles
OCL (5, 24)	5000	24284	29284	17467	0.40		vesicles
OCL (5, 30)	5000	29600	34600	24888	0.28		vesicles

The polydispersities of diblock copolymers was estimated using GPC calibrated with polystyrene standards. The block size of PCL was estimated from NMR spectroscopy. From this the re-defined size of the hydrophobic block (M_{CH2}) and f_{EO} were calculated as follows:

$$M_{CH2} = \frac{\text{MW of PCL x 82}}{114} \qquad f_{\text{hydrophilic}} = \frac{\text{MW of Diblock} - M_{CH2}}{\text{MW of Diblock}}$$

S2. Calculation of polymer amounts in Vesicles, Worm micelles, and Spherical micelles

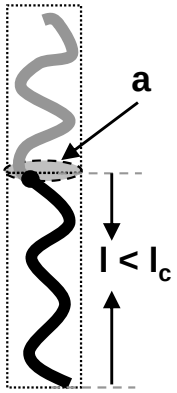

$$p = \frac{v}{a\,l}$$

p - packing paramater
a – interfacial area
l – length of hydrophobic tail
l_c – contour length of chain
v – core volume

vesicle

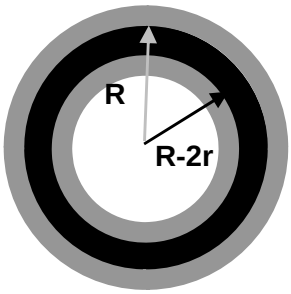

Surface Area:

$$4\pi R^2 + 4\pi (R-2r)^2$$

Molecules in a Vesicle of radius R

$$\frac{4\pi R^2 + 4\pi (R-2r)^2}{a}$$

cylinder

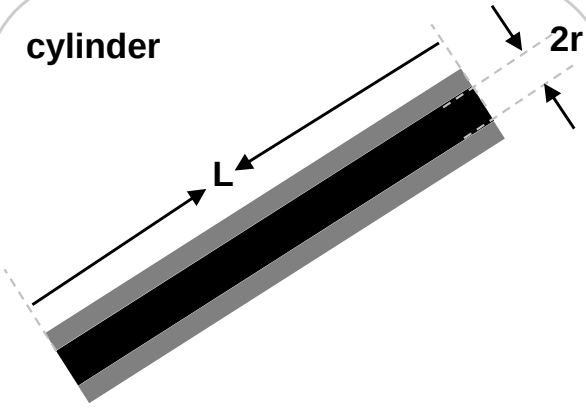

Surface Area:

$$2\pi r L$$

Molecules in a Worm of length (L):

$$\frac{2\pi r L}{a}$$

sphere

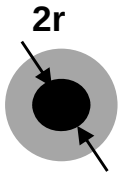

Surface Area:

$$4\pi r^2$$

Molecules in a Sphere:

$$\frac{4\pi r^2}{a}$$

S2A Calculation of polymer (and dye) amounts in Sphere micelles versus Vesicles

$$\frac{\text{Molecules in a Sphere of radius r}}{\text{Molecules in a Vesicle of radius R}} = \frac{4\pi r^2}{4\pi R^2 + 4\pi (R-2r)^2} = \frac{r^2}{[2R^2 - 4Rr + 4r^2]}$$

$$= \frac{1}{[2Z^2 - 4Z + 4]} \quad \text{where } Z = R / r \sim 100 \text{ for 2 } \mu\text{m Vesicle}$$

$$= \frac{1}{[20{,}000 - 400 + 4]} \sim \frac{1}{20{,}000} \quad \text{for 2 } \mu\text{m Vesicle}$$

$$\sim \frac{1}{160} \quad \text{for 200 nm Vesicle (sub-optical)}$$

$$\sim \frac{1}{6.5} \quad \text{for ~50 nm Vesicle (super sub-optical)}$$

If the dye:polymer ratio is fixed in images such as Fig.1A, then nano-Vesicles that are well below the diffraction limit from ~50 – 200 nm and equally unresolvable will nonetheless be much brighter than Spherical micelles.

S2B Calculation of polymer amount in Vesicles versus Worm micelles

$$\frac{\text{Molecules in a Worm of length R}}{\text{Molecules in a Vesicle of radius R}} = \frac{2\pi r R}{4\pi R^2 + 4\pi (R-2r)^2} = \frac{r R}{2\,[2R^2 - 4Rr + 4r^2]}$$

$$= \frac{Z}{2\,[2Z^2 - 4Z + 4]} \quad \text{where } Z = R / r \sim 100 \text{ for 2 } \mu\text{m Worm}$$

$$= \frac{100}{2\,[20{,}000 - 400 + 4]} \quad \text{for } Z = 100$$

$$\sim \frac{1}{400} \quad \text{for 2 } \mu\text{m Worm and 2 } \mu\text{m Vesicle}$$

$$\sim \frac{1}{100} \quad \text{for 8 } \mu\text{m Worm versus 2 } \mu\text{m Vesicle}$$

The mass of polymer in a single 2 μm vesicle equals the mass of polymer in one-hundred 8 μm worm micelles.

S3. AFM In-liquid imaging of OCL (2, 7) worms

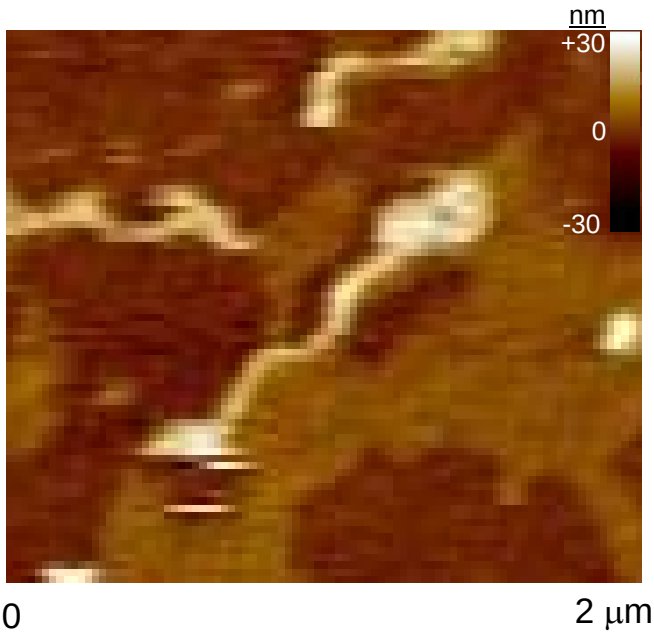

Worm micelle height: ~20 nm

Worm micelles were immobilized on surface of glass slide and imaging was done in PBS.

S4. Morphologies of PEO-b-PCL diblock copolymers by fluorescence microscopy

Morphologies of OCL assemblies were identified using fluorescence microscopy. The images in Figure S4 below, show the morphologies of various OCL polymers investigated. The concentration of polymer is 100 μM. Imaging was done after labeling the assemblies with a hydrophobic dye (PKH26, Sigma). The dye to polymer ratio is 1:100. Scale bar in all images below is 10 μm.

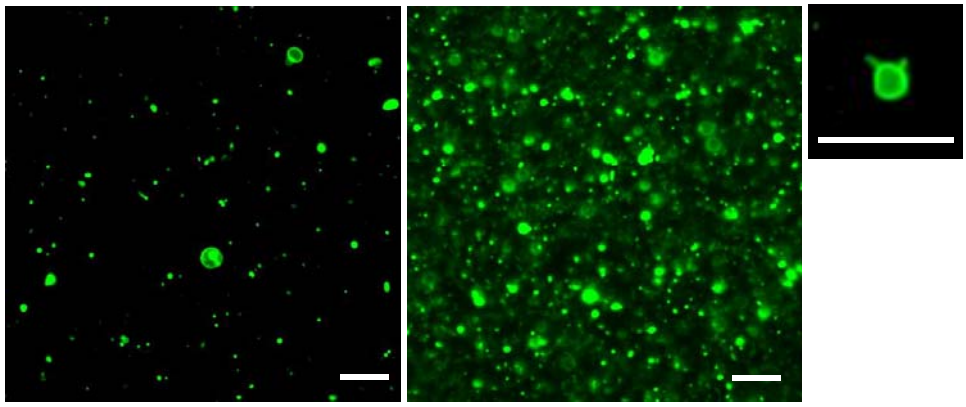

A. OCL (1, 3) Mostly vesicles

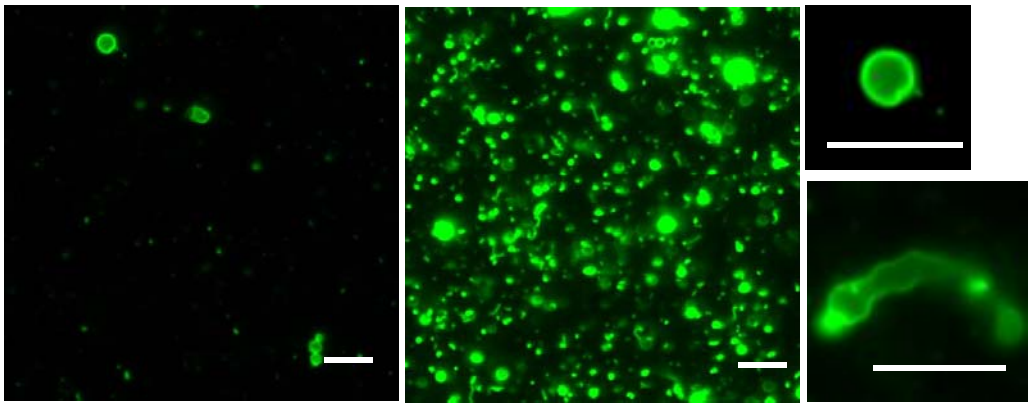

B. OCL (1, 4) Mostly vesicles and very few worms

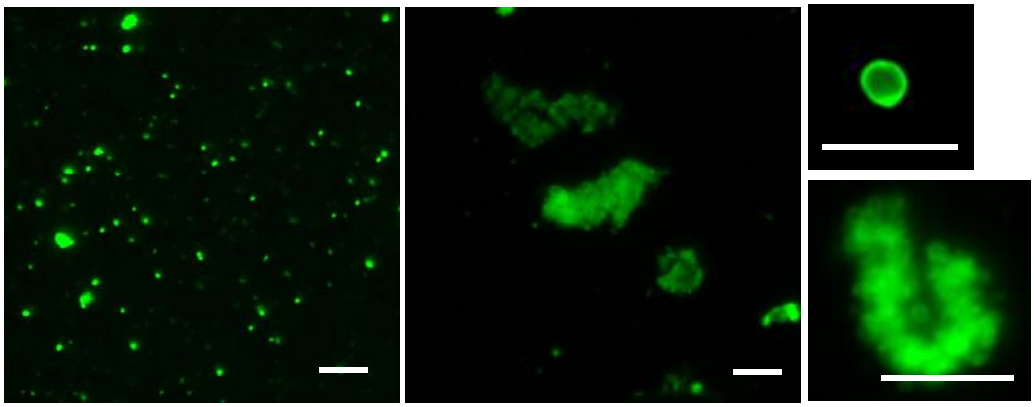

C. OCL (1, 6) Mostly vesicles and vesicle aggregates

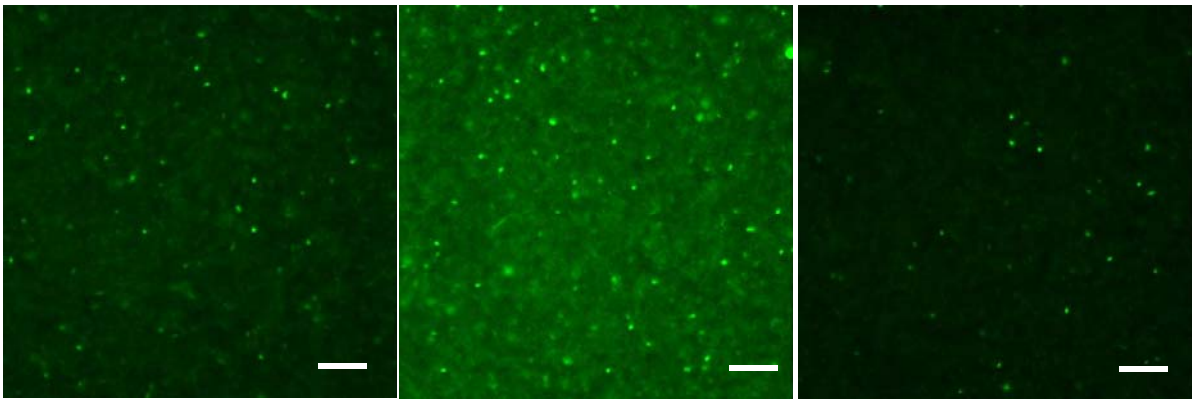

D. OCL (2, 3) Spherical micelles

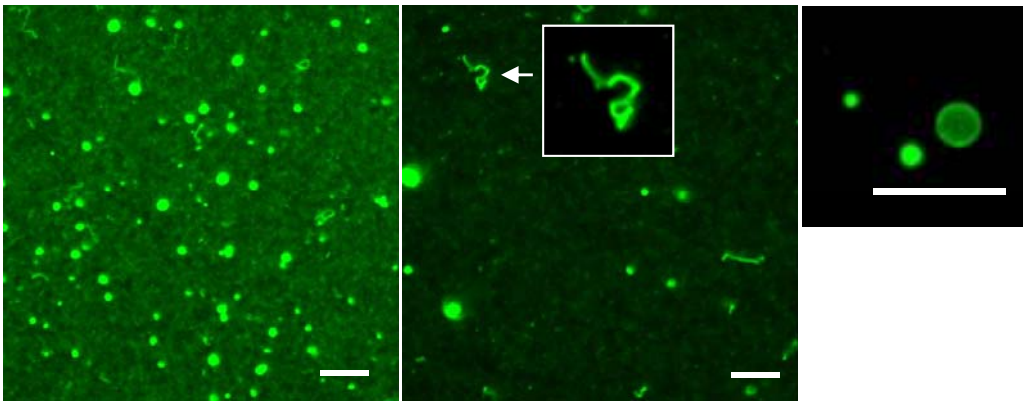

E. OCL (2, 6) Mixture of vesicles and worms

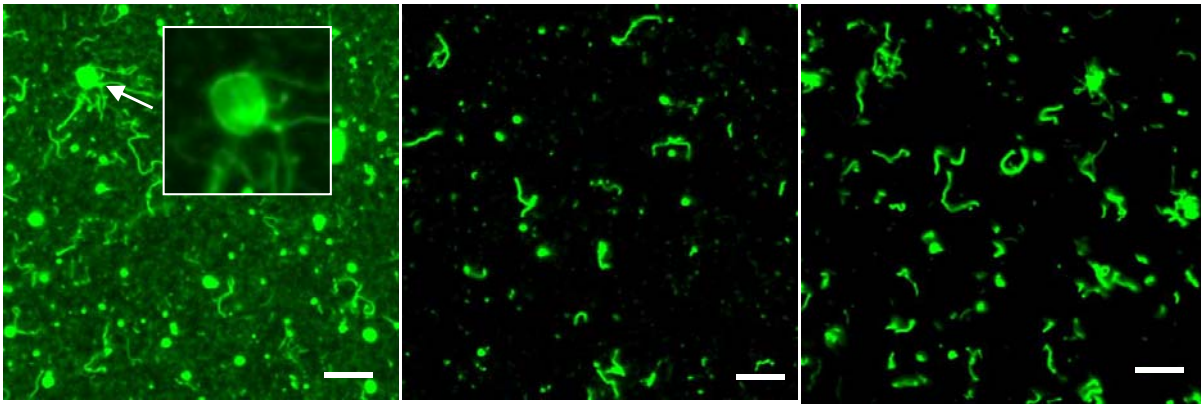

F. OCL (2, 9) Mixture of worms and vesicles

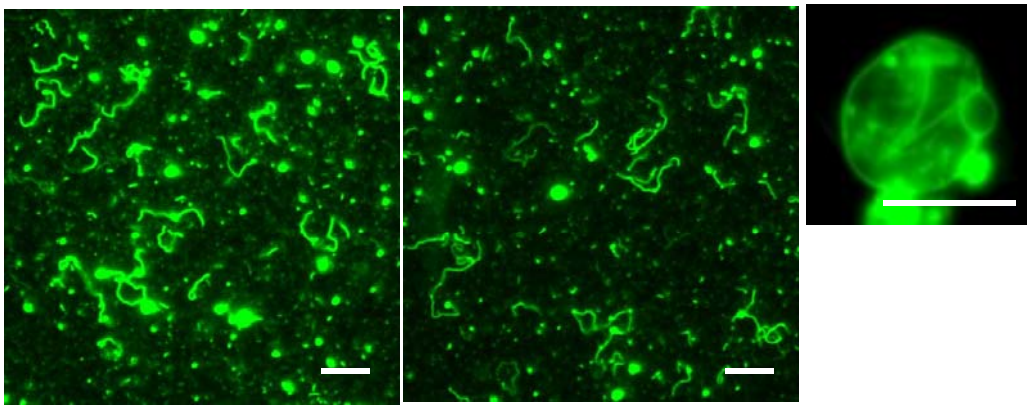

G. OCL (2, 12) Mixture of worms and vesicles

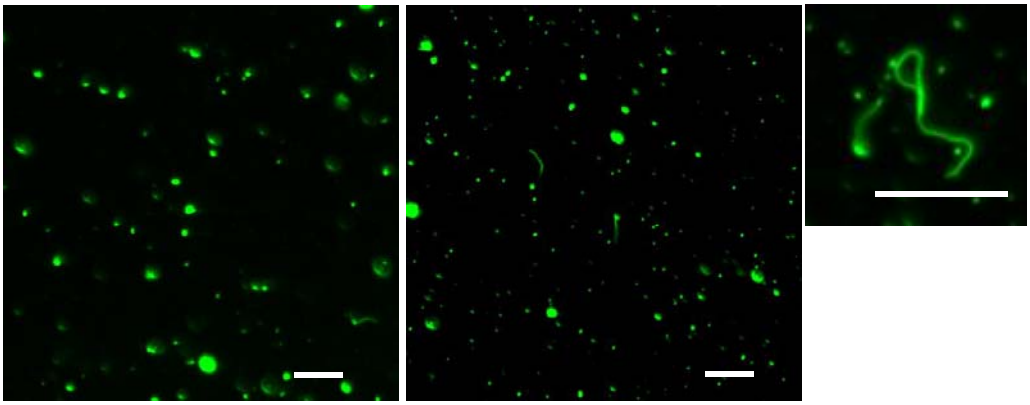

H. OCL (2, 13.5) Mostly vesicles and very few worms

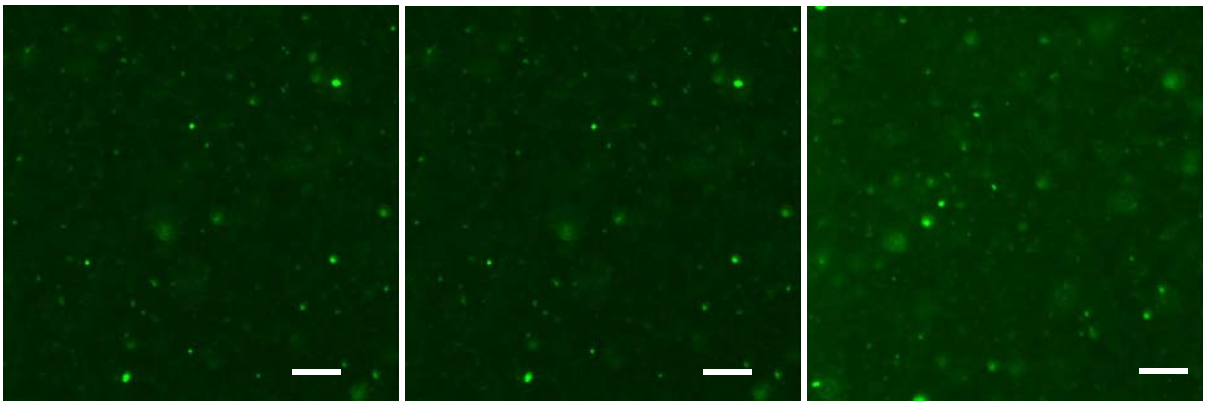

I. OCL (3.5, 6) Spherical micelles

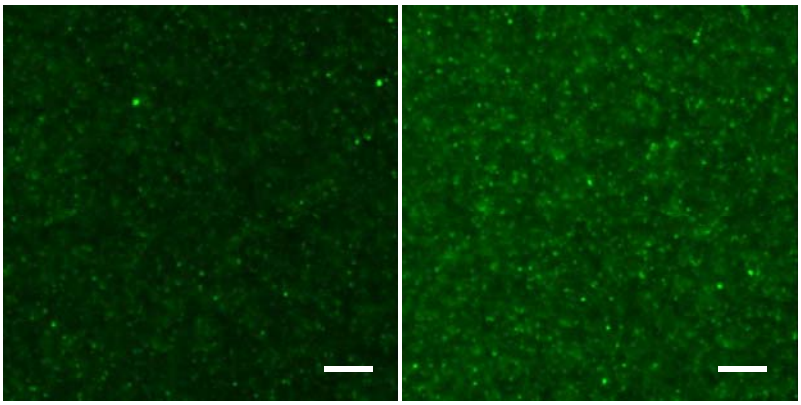

J. OCL (3.5, 9) Spherical micelles

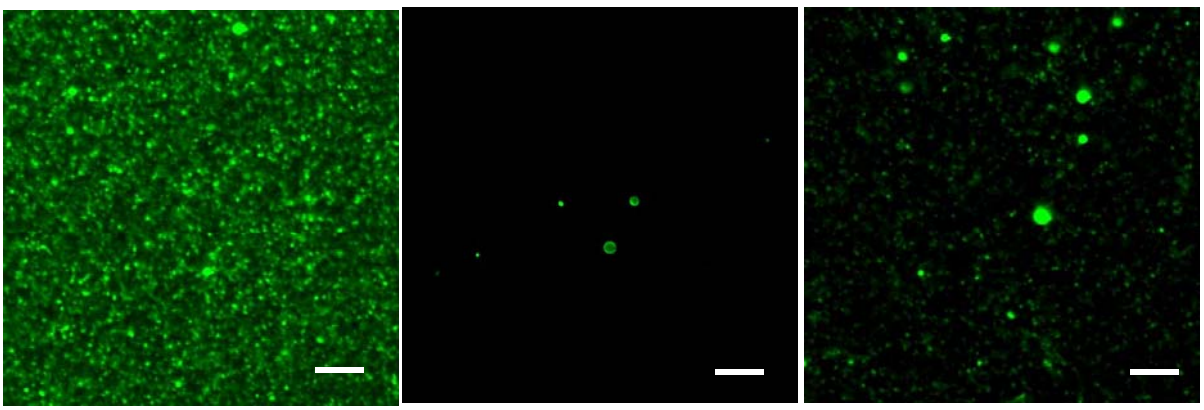

K. OCL (3.5, 12) Vesicles and spherical micelles

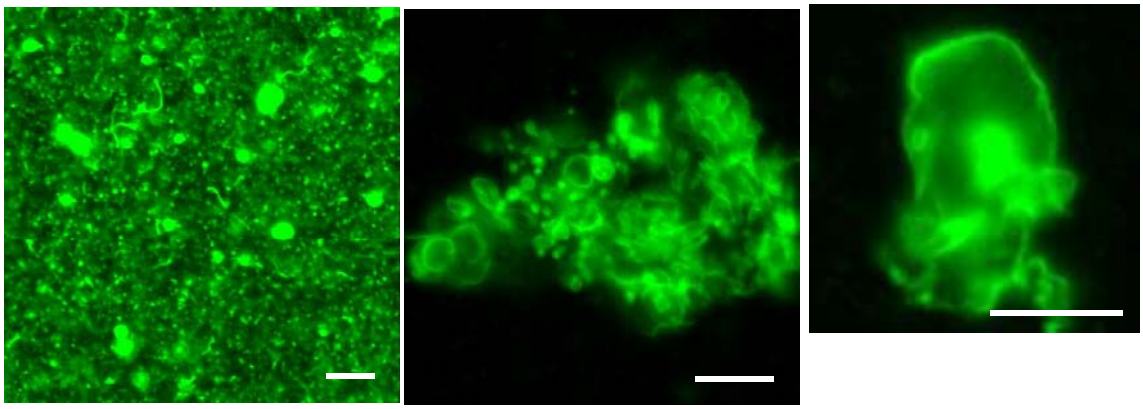

L. OCL (3.5, 15) Mostly vesicles, vesicle aggregates and few worms

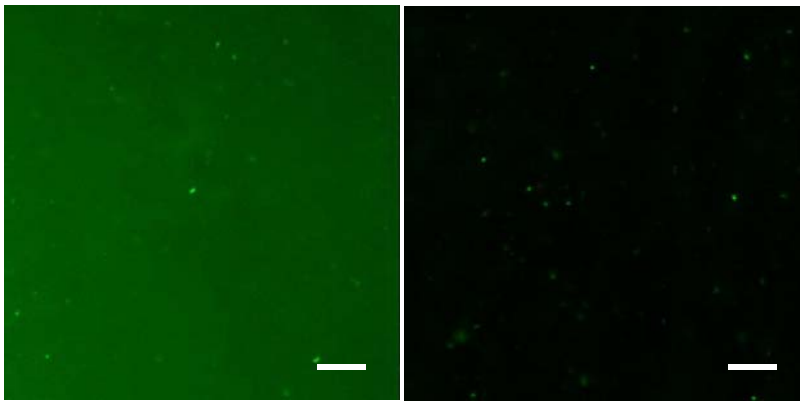

M. OCL (5, 3) Spherical micelles

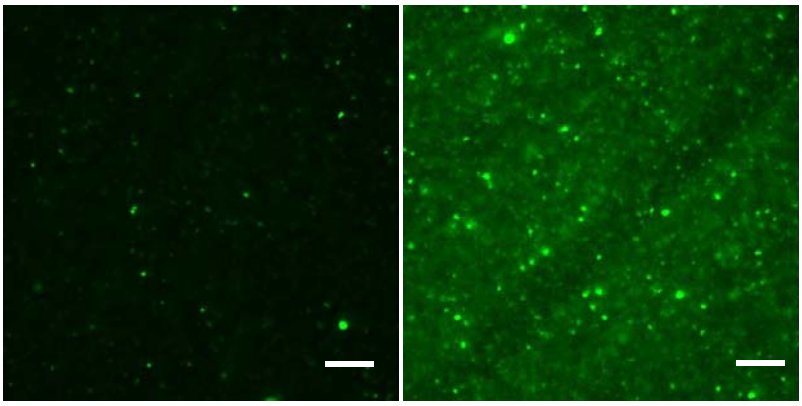

N. OCL (5, 6) Mostly spherical micelles

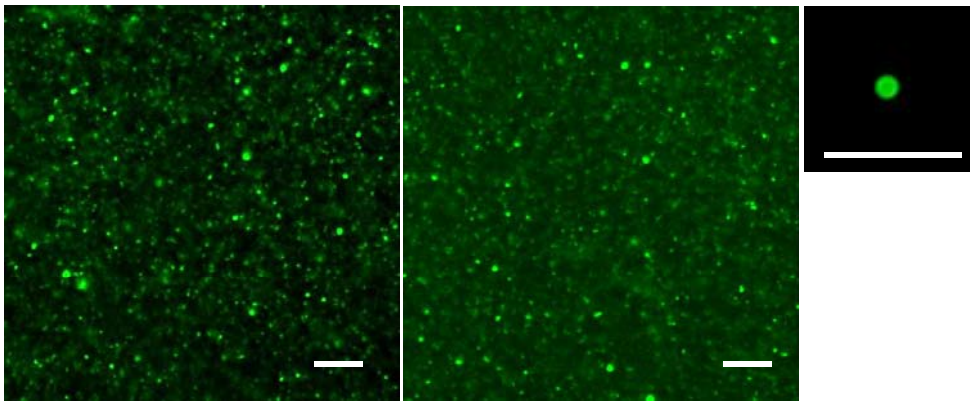

O. OCL (5, 9) Mostly spherical micelles and very few vesicles

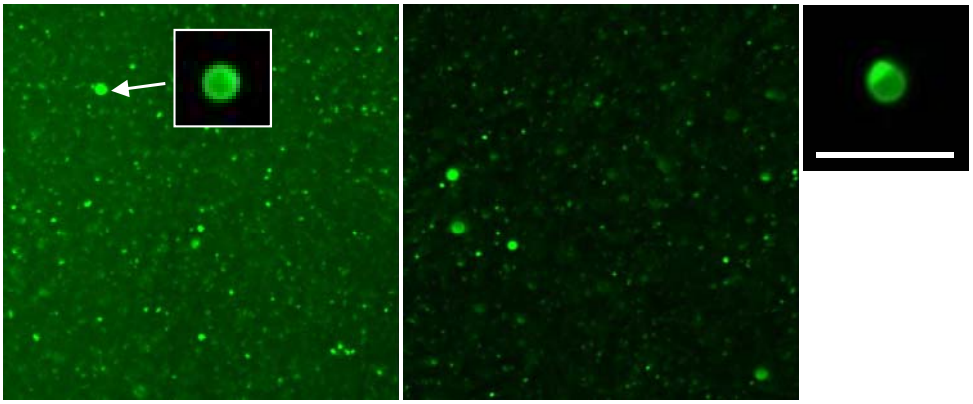

P. OCL (5, 12) Vesiclces and spherical micelles

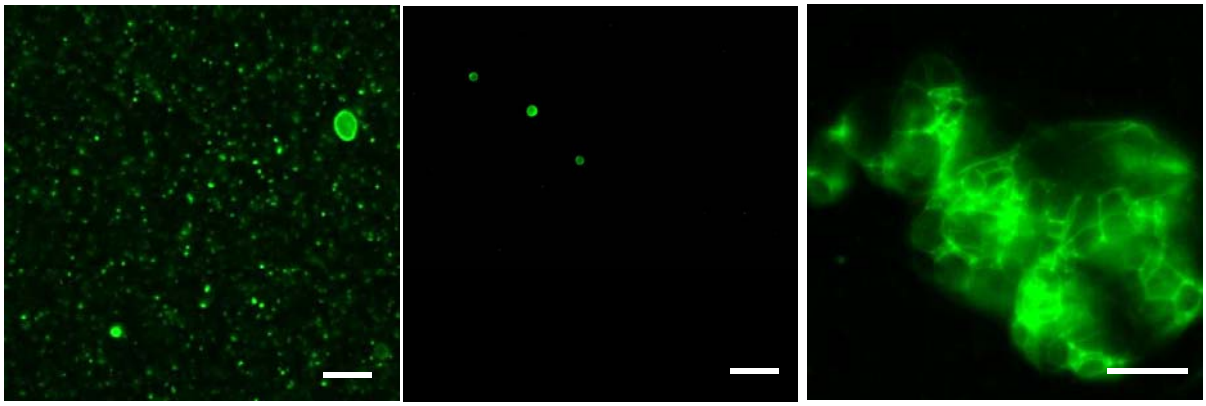

Q. OCL (5, 18) Vesicles and vesicle aggregates

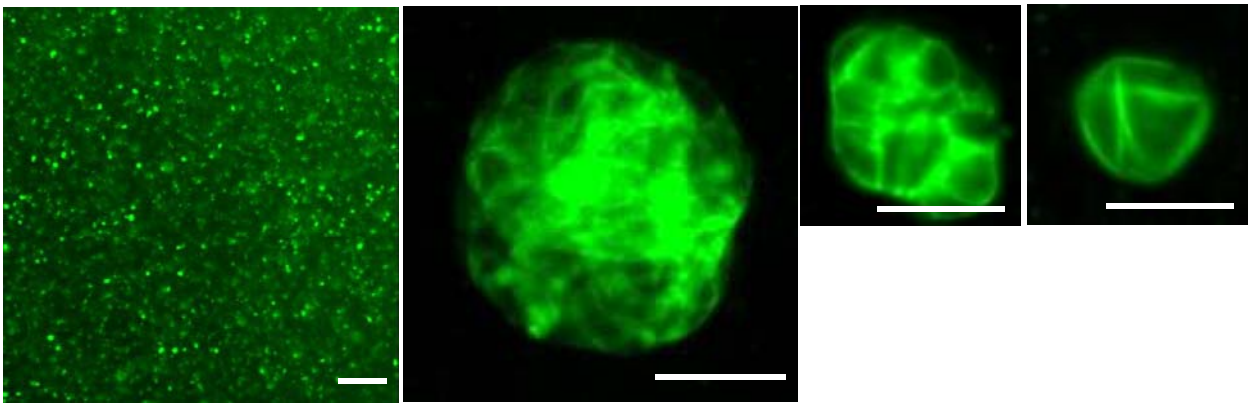

R. OCL (5, 24) Vesicles and vesicle aggregates

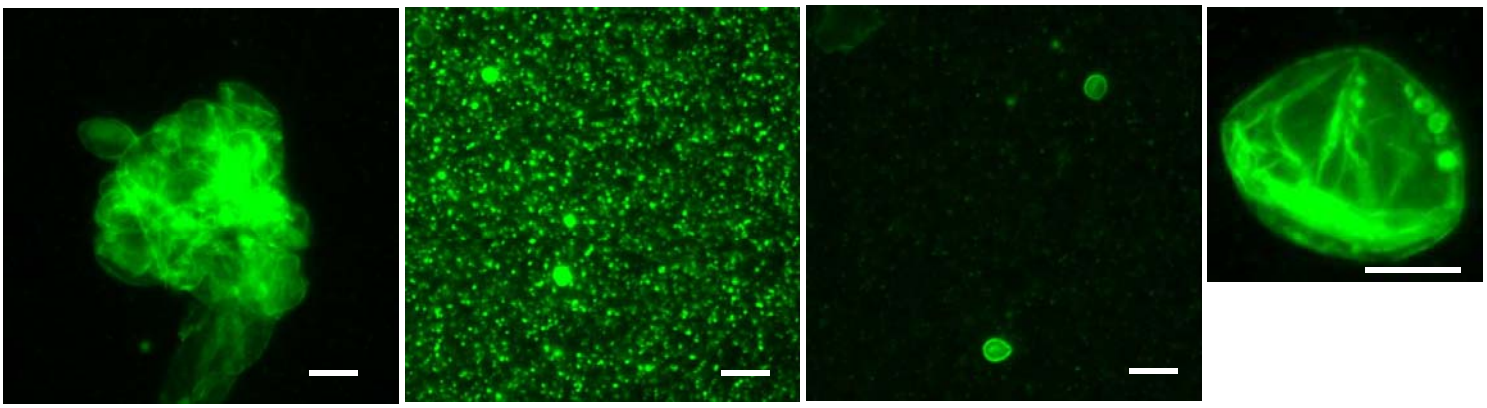

S. OCL (5, 30) Mostly vesicles, vesicle aggregates and some giant vesicles

S5. Calculation of χ

The chi values were calculated from short chain atomistic simulations of polymers in the melt phase. The volume of the monomer, V_m in the melt phase was estimated from molecular dynamics simulations of PEO, PCL, and PBD using potentials based of the CHARMM27 force field at 293K. The smallest monomer volume of the two respective polymers is used by convention. The difference in Hildelbrand solubility parameters was used to calculate χ. δ_i and δ_j are the Hildebrand solubility parameters of the two polymer blocks, PEO and PCL or PBD.

$$\chi = \frac{V_m}{k_B T(\delta_i - \delta_j)^2}$$

The estimated monomer volume (V_m) for PEO is 41.4 cm^3/mol, for PCL is 59.9 cm^3/mol and for PBD is 31.1 cm^3/mol. The approximate Hildebrand solubility parameter (δ) in units of cal/cm^3 for PEO is 14.1, for PCL is 11.2 and for PBD is 9.00 (Liu 2004).

Liu, J. Xiao, Y, and Allen X. Polymer-Drug Compatbility: A Guide to the Development of Delivery Systems for the Anticancer Agent Ellipticine. *Journal of Pharmaceutical Sciences*. 93, 132-143 (2004).

.

S6. Characterization of Low MW OCL Assemblies

S6A. OCL (1, 3)

Dynamic Light Scattering (DLS)

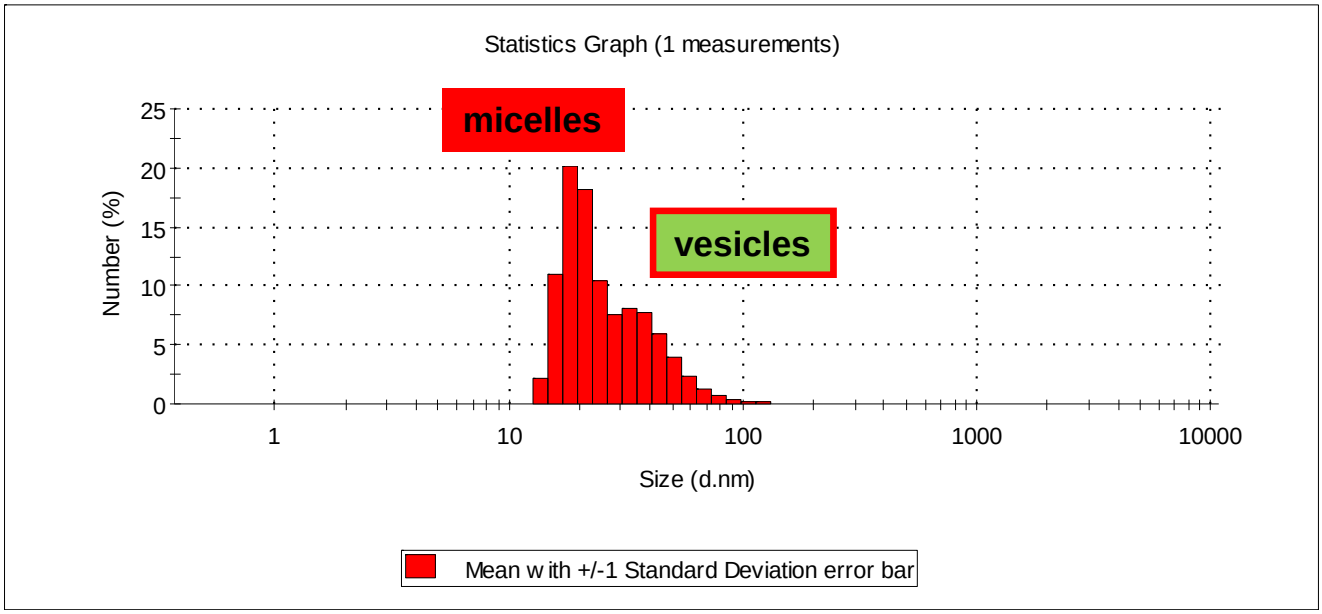

Fluorescence Microscopy Image

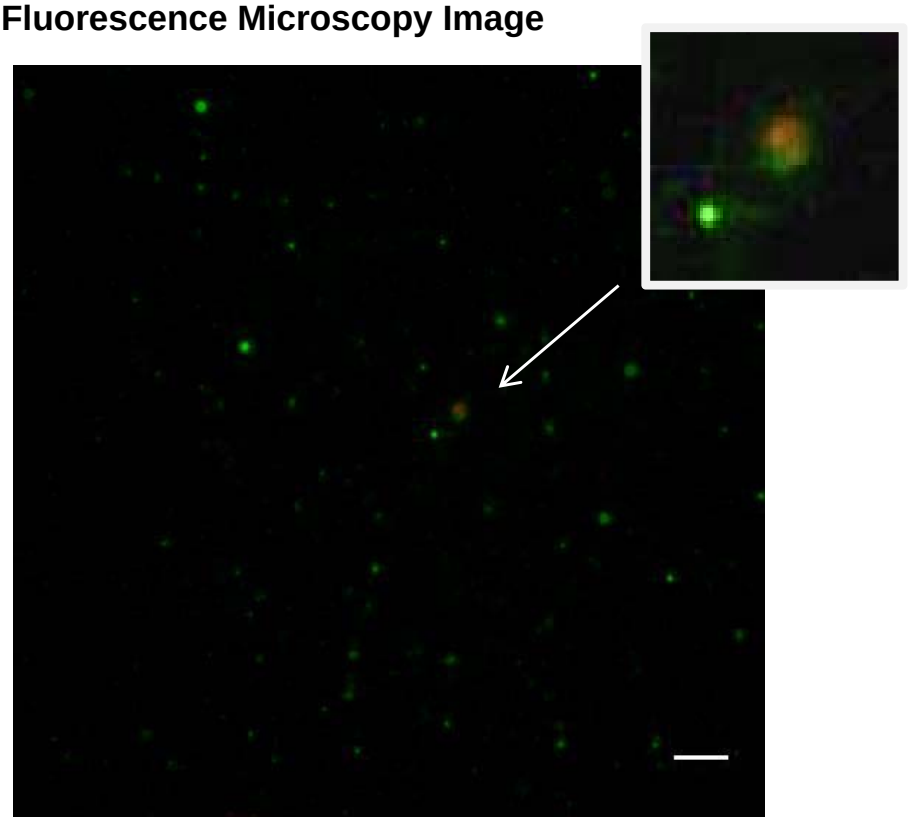

Samples were prepared with FITC dextran (4 kD) and extensively diayzed before imaging.
Localization of FITC dextran after extensive dialysis suggests formation of vesicles.
Vesicle formation is evident from the two color micrographs showing internalization of FITC dextran within the lumen.

S6B. OCL (1, 1)

Dynamic Light Scattering (DLS)

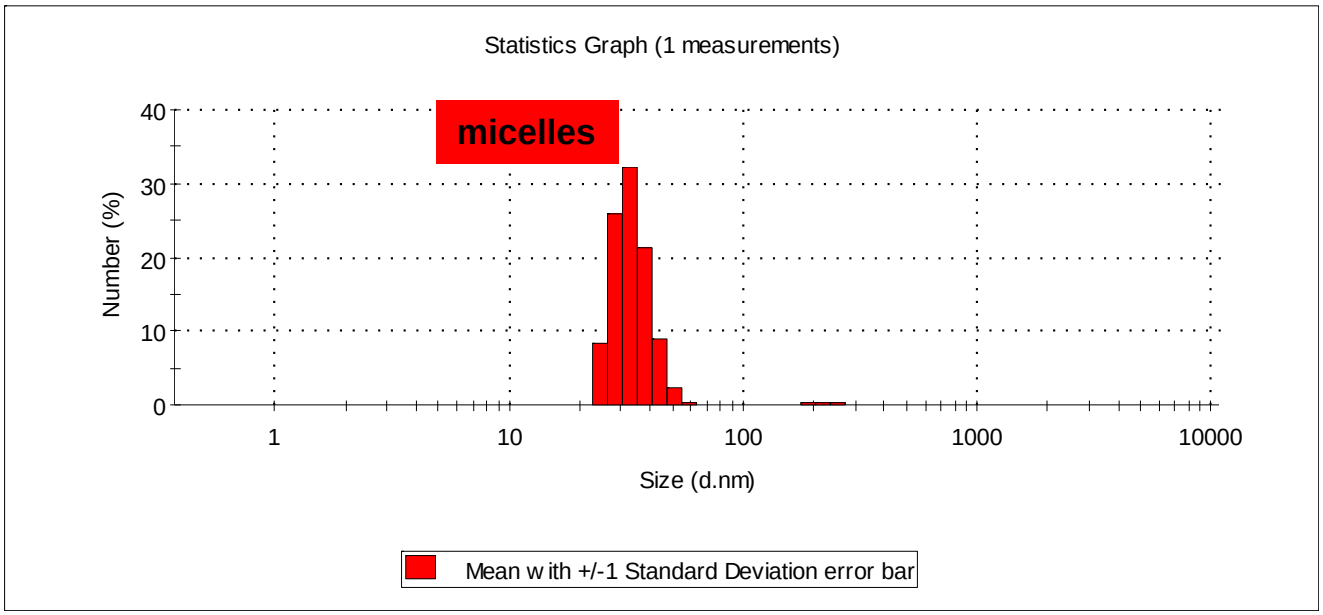

Fluorescence Microscopy Image

OCL (1, 1)

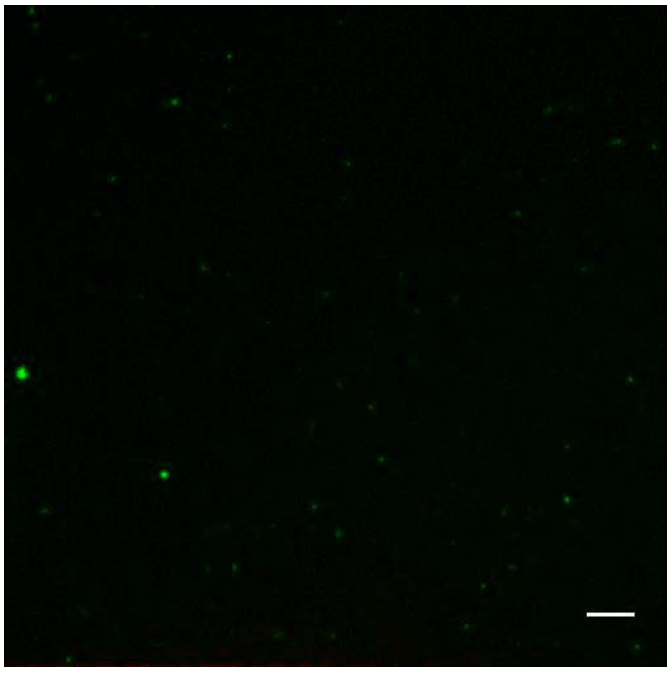

OCL (1, 0.5)

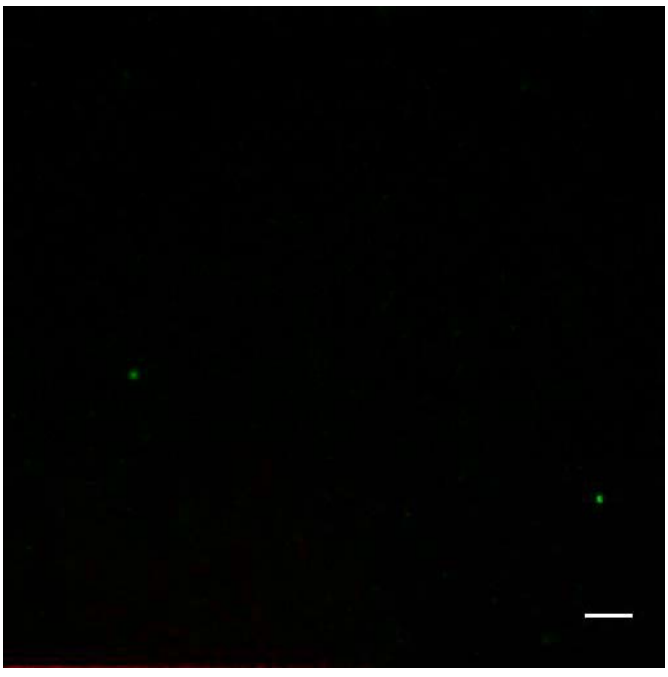

Samples were prepared with FITC dextran (4 kD) and extensively diayzed before imaging.
Two color imaging shows no FITC dextran in sample suggesting absence of vesciles.

S7. Video of OCL (2, 9) sample

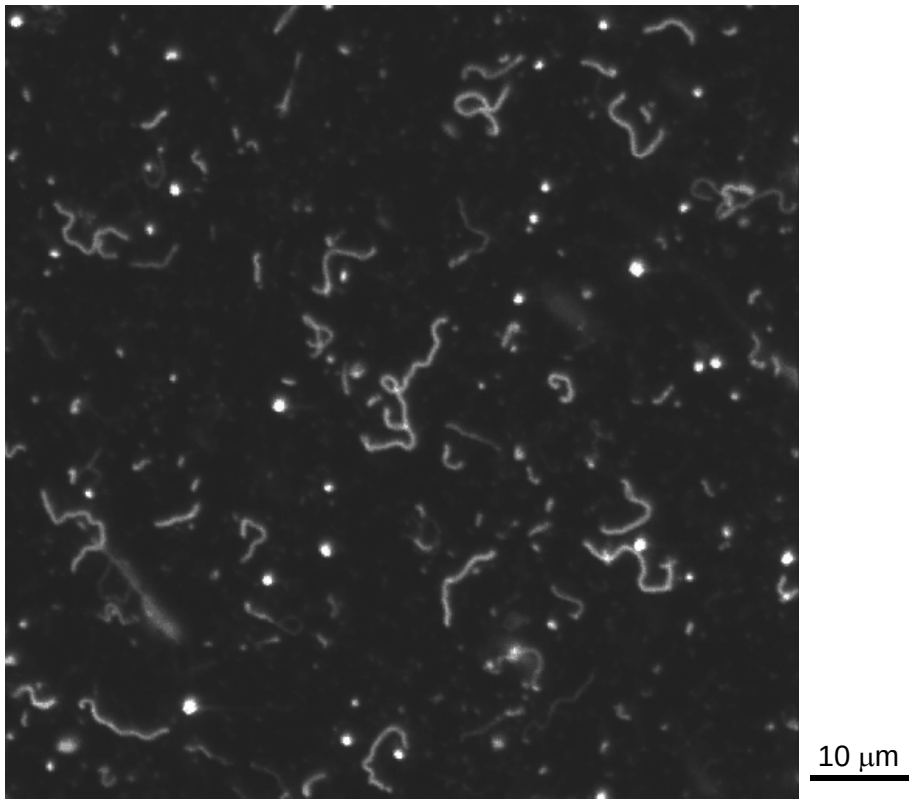

Figure S7. Time lapse fluorescence video microscopy of a solution of OCL(2,9) worm micelles. From the above movie a total of 51 worms were counted, out of which 4 were rigid. On an average from 10 such movies the percentage of rigid worm micelles counted were approximately 10%.

S8. Video of OCLA (2, 7.4, 1.6) sample

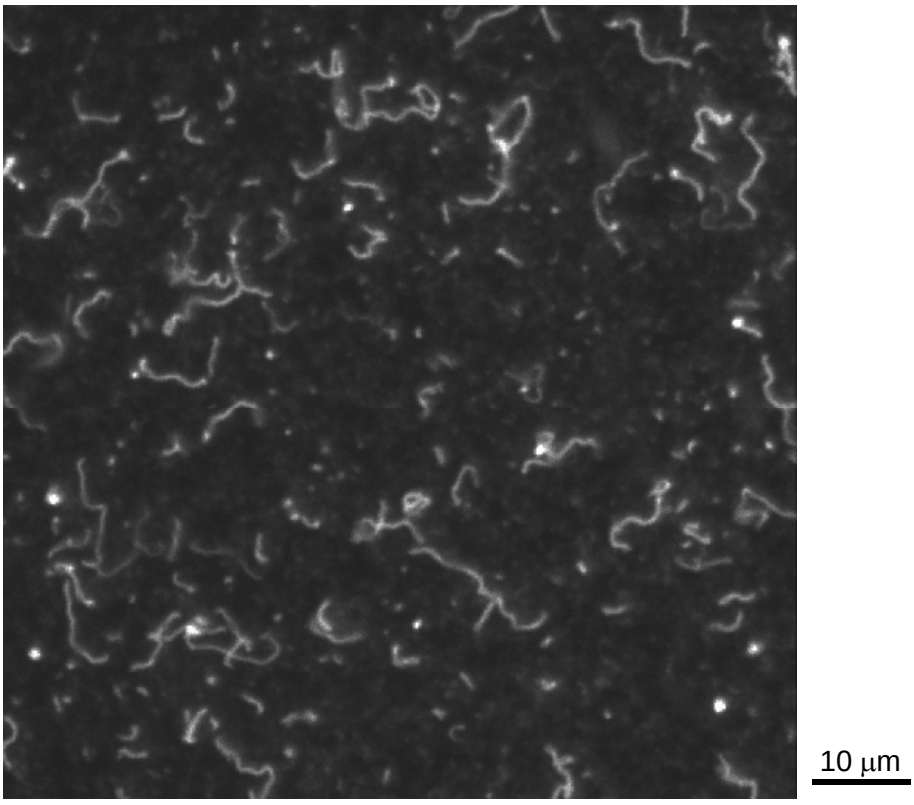

Figure S8. Time lapse fluorescence microscopy of a solution of OCLA (2,7.4, 1.6) worm micelles. From the above movie a total of 80 worms were counted out of which none were rigid. No rigid worm micelles were detected from 10 such movies.

S9. Video of OB (4, 6) sample

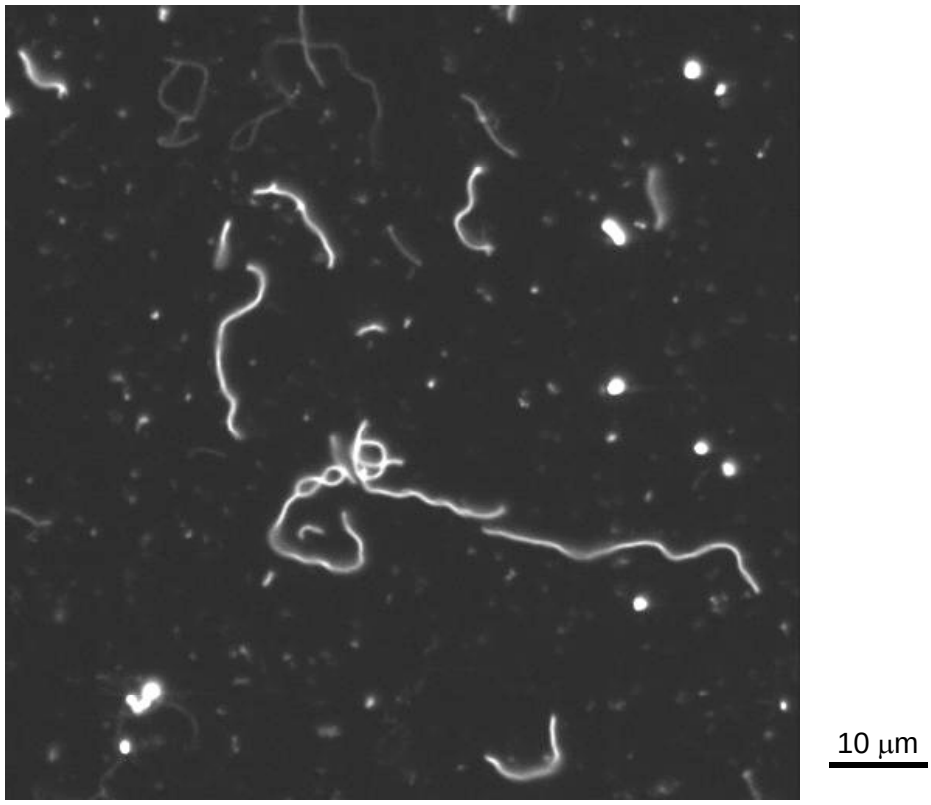

Figure S9. Time lapse fluorescence microscopy of a solution of OB (4, 6) worm micelles. No rigid worm micelles were detected in OB samples.

S10. Measurement of persistence length at different concentrations of dye for OCL (2, 6)

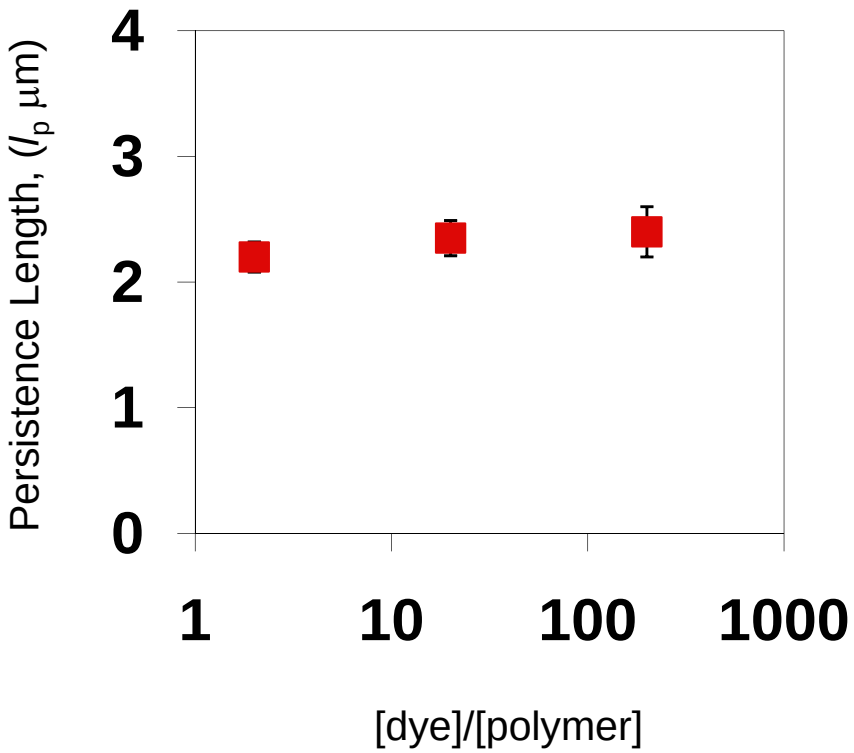

Figure S10. The persistence length of OCL (2, 6) worm micelles as a function of dye concentration is shown. The persistence does not vary as the concentrations of dye is varied indicating that the dye is minimally perturbing to the worm flexibility.

S11. Measurement of persistence length of OCL (2, 6) and OCL (2, 9)

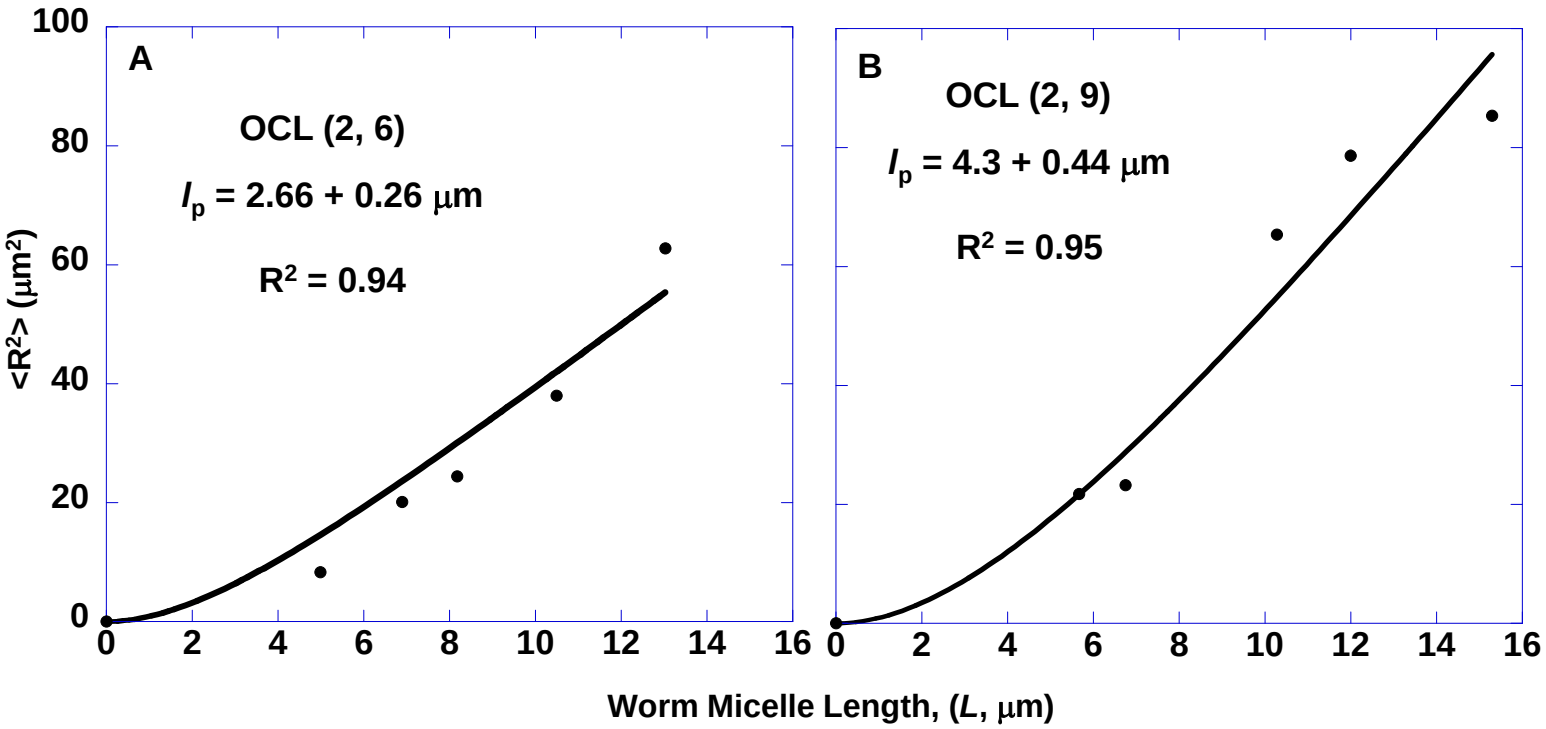

Figure S11. Persistence length measurement of **A.** OCL (2, *L*6) and **B.** OCL(2, 9) worm micelles. The persistence length was obtained by fitting the <R²> vs data to a worm-like chain model defined by $\langle R^2 \rangle = 2(l_p)^2 [(L/l_p) - 1 + exp(-L/l_p)]$, where R is the end-to-end distance and L is the contour length.

S12. Analyses of lipid results from Evans et al. and Rawicz et al. *Biophys. J.* (2000)

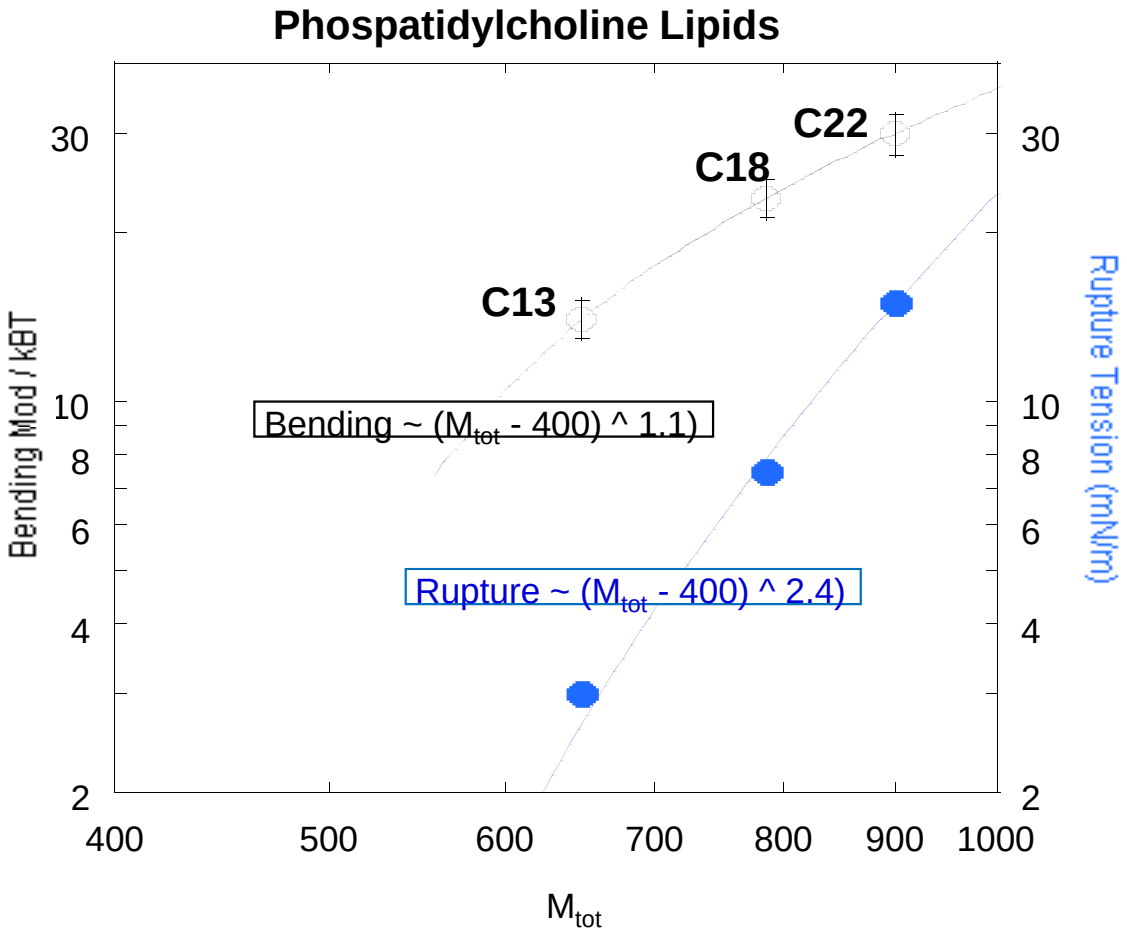

S13. Measurement of worm micelle contour lengths

Flourescence microscopy image of a solution of worm micelles is shown in Figure S8A. The procedure for sample preparation, imaging and measurement of contour lengths is described below.

Sample preparation for imaging

100 μL of 100 μM worm solution is taken in an eppendorf tube. To this 0.2 μL of 0.2 mM dye (PKH26, Sigma) is added, gently mixed and then diluted to 250 uL with DI water. To this solution 25 μL of 10 mM NaCl solution is added and gently mixed. From this, 3 μL is spotted on a glass slide and a 25 MM square cover slip is placed on top and pressed to spread the worm solution. After two minutes the glass slide is placed on a Nikon Fluorescence microscope and imaged using a CCD camera (Figure S8B). If the worm micelles are touching one another or if they are not fully immobilized on the glass surface, their concentration as well as the concentration of salt are appropriately adjusted.

Measurement of contour lengths

The microscopy image of immobilized worm micelles shown in Figure S8B. The image is first filtered with a symmetric Laplacian of Gaussian (LoG) filter with a standard deviation of 1.5 pixels to suppress background noise. The gamma value of the image is then adjusted to be between 0.6 and 0.8. Using a stretched LoG filter with a standard deviation of the minor axis of 1.5 pixels and a long axis of roughly 12 pixels, a battery of filters of varying angles is constructed and the image is serially filtered with each of the angle LoG filters. At each pixel, the maximum response of the stack of angled LoG filters is used to assemble a new image that emphasizes the line-like features of the subject image. The line-like image is thresholded using a Matlab function that creates a binary image and minimizes the standard deviations of the foreground and background pixel intensities. Once the image is thresholded in this manner, objects that are clearly not worms are removed. This includes objects with holes larger than 1 pixel, objects with a major elliptical axis of less than 12 pixels, and objects that are not completely removed by eroding with a diamond of diameter 4 pixels. All objects touching edges are removed. The image is then converted into a skeleton representing worm backbones as shown in Figure S8C. At this point, it is important to remove worms that are overlapping, as it is not possible to determine which extensions belong to which worms. First, each object is parsed to determine the number of intersections. Small spurs of less than 6 pixels are removed as these tend to be artifacts. Any branched objects that remain are discarded. The lengths of all remaining skeletons are computed. Since the number of worm micelles counted differs for each sample the frequency is normalized and plotted as shown in Figure S8D. The output of segmented images were manually checked for any false positives. Typically, the false positives are less than 5%. For estimating the average contour length of a sample of worm micelle solution, 20 random images of immobilized worm micelles are captured and the contour length distribution is computed.

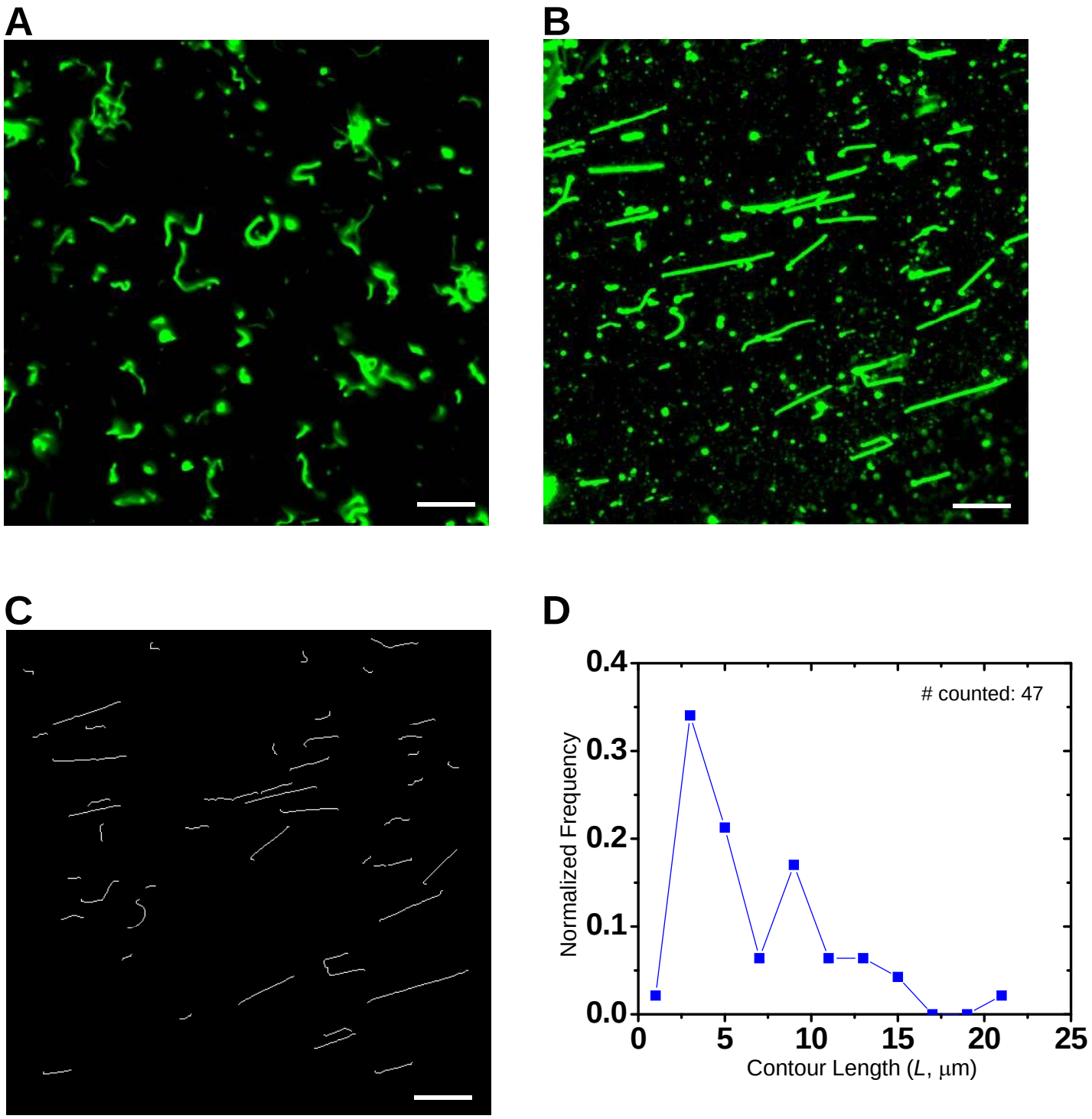

Figure S13. A. The fluorescence microscopy image of a solution of dye (PKH26, Sigma) labeled OCL (2, 9) worm micelles is shown. The dye to polymer ratio is 1:100. **B.** The worms are immobilized on glass surface after adding ~7 mM NaCl. **C.** The skeletonized image obtained by processing the image in **B** using a Matlab function is shown. **D.** The normalized contour length distribution of worm micelles within a single frame (Figure **C**) is shown. Scale bar in all images is 10 μm.

S14. Micropipette aspiration and rupture of OCL vesicles

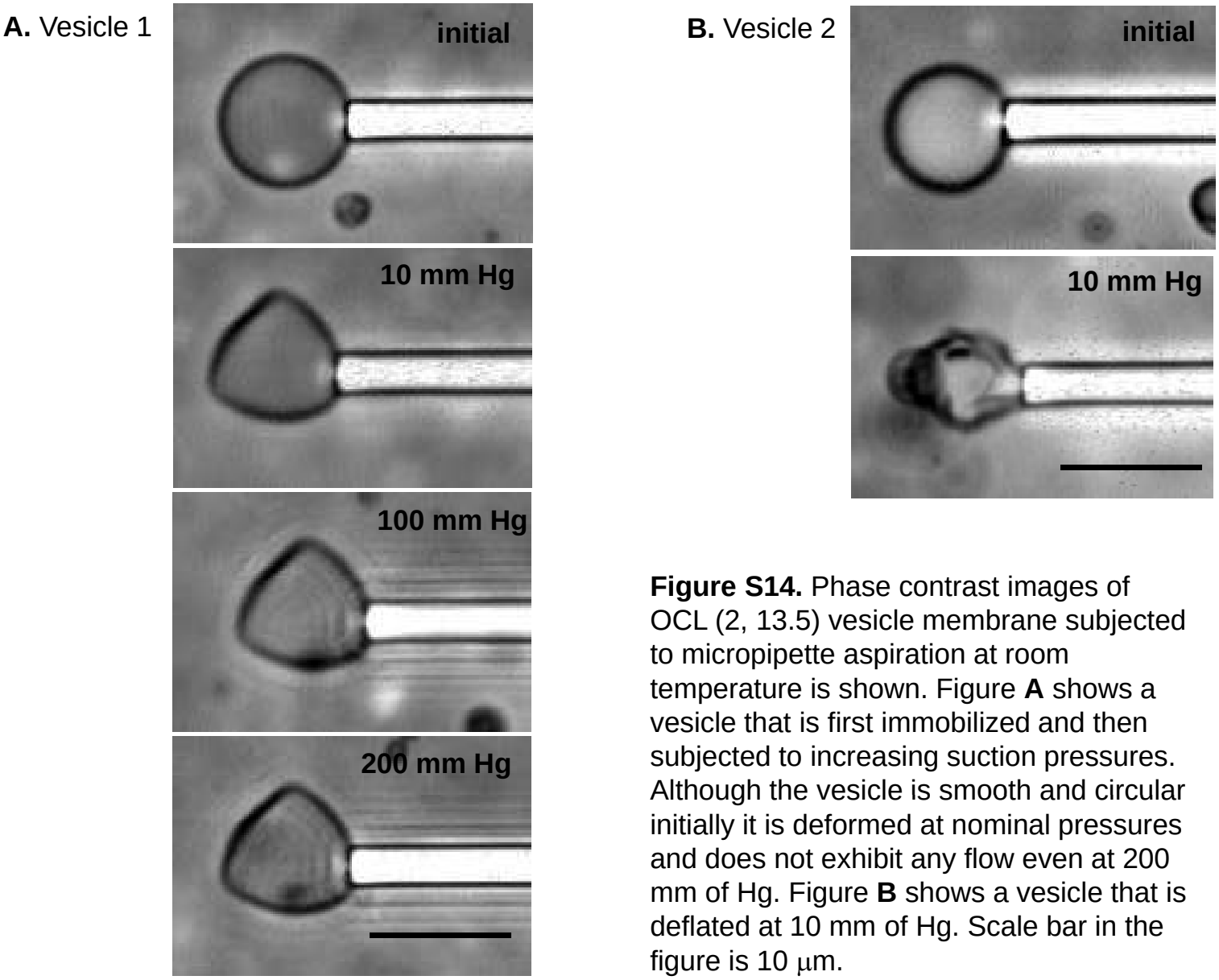

Figure S14. Phase contrast images of OCL (2, 13.5) vesicle membrane subjected to micropipette aspiration at room temperature is shown. Figure **A** shows a vesicle that is first immobilized and then subjected to increasing suction pressures. Although the vesicle is smooth and circular initially it is deformed at nominal pressures and does not exhibit any flow even at 200 mm of Hg. Figure **B** shows a vesicle that is deflated at 10 mm of Hg. Scale bar in the figure is 10 μm.

S15. Temperature dependent stability of OB worm micelles

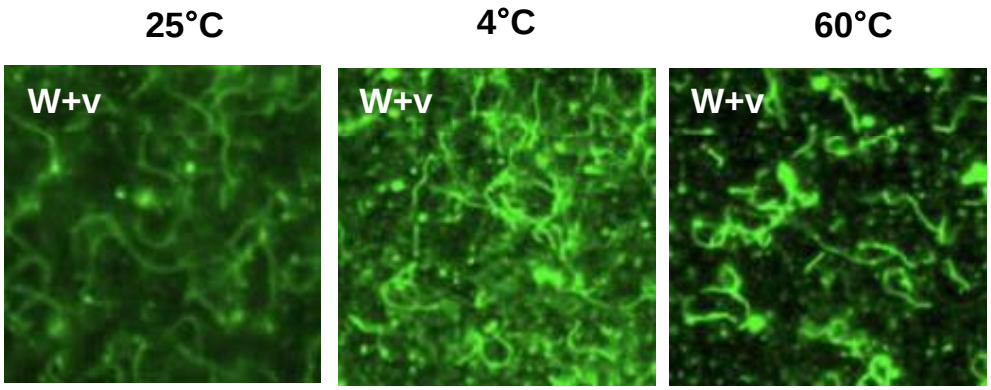

Figure S15. Fluorescence microscopy images OB (4, 6) samples at different temperatures. OB worm micelles were prepared by solvent evaporation method at room temperature and imaged after equilibrating at 4°C, 25°C and 60°C for a day. The images above indicate no change in OB morphologies as a result of heat treatment.